MEASUREMENTS OF RELATIVE PERMEABILITY FOR STEAM-WATER FLOW IN POROUS MEDIA

A REPORT
SUBMITTED TO THE DEPARMENT OF
PETROLEUM ENGINEERING OF STANFORD UNIVERSITY
IN PARTIAL FULFILLMENT OF THE REQUIREMENTS FOR
THE DEGREE OF
MASTER OF SCIENCE

By
Raul A. Tovar
June 1997

Acknowledgments

I would like to thank Dr. Cengiz Satik for his continuos encouragement and guidance in this research project. I am also very obliged to my principal advisor, Dr. Roland Horne for his support and invaluable insights.

Financial aid for this work was provided by the Department of Energy under contracts DE-FG07-90ID12934 and DE-FG07-95ID13370 and the Geothermal Industrial Affiliates. Their support is gratefully acknowledged.

Last but not least, a very special thanks to my wife for her patience and understanding.

Abstract

This report describes experimental efforts towards obtaining relative permeability for steam-water flow in a homogeneous porous medium under adiabatic steady-state conditions. The porous media used in the experiments were Berea sandstone core samples. Porosity and saturation distribution were measured using a high resolution X-ray computer tomography (CT) scanner. Steam fractional flow, crucial in evaluating relative permeabilities, was monitored using a computer data acquisition system for measuring temperatures, pressures and heat fluxes. In particular, two approaches were investigated: (1) the simultaneous injection of steam and water and (2) the injection of water while it goes through a phase change. Both methods required assumptions with respect to two-phase flow and heat transfer, which lead to uncertainty in the results. Nonetheless, injecting through a single line greatly simplified the experiments.

In addition, the variation of absolute permeability with respect to changes in temperature and flow rate were investigated. The results indicated that absolute permeability is practically independent of temperature and flow rate.

Table of Contents

List of Tables and Figures

Section 1
Introduction

Darcy's law defines the absolute permeability of a porous medium completely saturated with a fluid as constant irrespective of the nature of the fluid flowing through it. The need for a relationship between two fluid phases, such as water and steam, flowing simultaneously through a porous medium gives rise to the so-called effective permeability. In this case part of each of the fluids remains immobile in the porous medium restricting the mobility of the other fluid. This effective permeability can be normalized with respect to the absolute permeability to obtain a dimensionless factor that is called the relative permeability of the particular fluid flowing in the presence of another fluid. Relative permeabilities are important in reservoir studies because they are needed as input parameters for reservoir simulation in order to match or forecast reservoir production performance. In particular, steam-water relative permeabilities are of concern to geothermal reservoir studies since steam and water are responsible for the transport of reservoir heat. Empirical measurements of relative permeabilities depend on the saturation of each fluid. The steam and water phases are easily transposable from one phase to the other by boiling or condensation, making it difficult to measure the respective phase flowing fraction.

Different techniques have been used in the past to obtain a relationship between relative permeability and saturation. One of the earliest experimental attempts was carried out by Arihara, in 1974. Another approach has been to use the producing history of a geothermal reservoir to obtain steam-water relative permeability (Grant, 1977; Horne and

Ramey, 1978). Ambusso (1996) reported a set of curves that used a computer tomography (CT) scanner to obtain the saturation distribution along an experimental core sample. Unfortunately not all of the previous studies are consistent perhaps due to the lack of reliable and accurate saturation measuring equipment.

The motivation behind our experiments is the improvements made possible by modern data acquisition equipment. Reliable temperature, pressure and heat flux measurements crucial in determining the fractional flow of each phase were obtained by using data acquisition software and hardware that collects, analyzes and stores data in a personal computer. Accurate measurements of water saturation were obtained by using a high resolution X-ray computer tomography (CT) scanner.

Experiments in the past have used either unsteady-state methods or steady-state methods. These methods can be accomplished either by injecting liquid water that undergoes a phase change in the porous medium or by simultaneous injection of steam and water into the porous medium. This report presents the procedure and results of these last two approaches under steady-state conditions to obtain an empirical correlation between the relative permeability of steam-water flow in porous medium and the water saturation. In addition, we investigated the variation of absolute permeability with respect to temperature and flow rate as reported by Trimble and Menzie (1975) and Ambusso (1996) respectively.

Section 2

Literature Review

Darcy's law is used in petroleum, groundwater and geothermal studies to describe flow through a homogeneous porous medium. For two-component two-phase flow, an empirical variation of Darcy's law has been established. This variation introduces the concept of relative permeability as a function of the saturation of each component. The commonly assumed relative permeabilities for homogeneous media are the Corey expressions (Corey, 1954):

$$
\begin{aligned}
k_{rl} &= S^{*4} && (S^* < 1) \\
k_{rg} &= \left(1 - S^*\right)^2 (1 - S^{*2}) && (S^* < 1) \\
S^* &= \left(S - S_{lr}\right) \Big/ \left(S_{gr} - S_{lr}\right)
\end{aligned}
\qquad (1)
$$

where S_{gr} and S_{lr} are the irreducible or residual saturations for liquid and gas, respectively.

These expressions are somewhat arbitrary, particularly so in geothermal systems (Piquemal, 1994). In general, relative permeabilities are obtained experimentally. The sum of the relative permeabilities is usually less than one as each phase obstructs the flow of the other. In the case of geothermal reservoirs or in enhanced oil recovery methods steam and water constitute a single-component two-phase flow, different from the more common case of a two-component two-phase flow. Difficulties are encountered when describing steam-water flow behavior because the vapor and liquid phases are

interchangeable by boiling or condensation. With only a slight change in enthalpy the phase distribution of the steam-water mixture will change (Trimble and Menzie, 1975). The two phases may distribute themselves differently in the porous medium than would a two-component flow of fluids like nitrogen and water. Nonetheless, experiments suggest that steam-water relative permeabilities are still a function of the saturation (Chen et al., 1978; Piquemal, 1994). Hence empirical measurements of relative permeability can be divided in two aspects: (1) the ability to measure the saturation and (2) the ability to determine relative permeability itself.

The methods used in determining relative permeability experimentally for two-phase, two-component flow were synthesized by Osoba et al. (1951) and Richardson et al. (1952). These methods were reviewed by Ambusso (1996). For steam-water relative permeabilities in one-component two-phase flow, obtaining the phase flowing fractions is most crucial and requires some modifications to the two-component, two-phase flow methods by the inclusion of conservation of energy. Experimentally, steam-water relative permeabilities are calculated from the core length Δx, cross sectional area A, fluid viscosities μ, injection rates and the differential pressure across the core section Δp using the following relations for water and steam respectively:

$$k_{rl} = -\frac{(1-x)m_t \mu_l \nu_l}{kA\dfrac{\Delta p}{\Delta x}} \tag{2}$$

and

$$k_{rs} = -\frac{x m_t \mu_s \nu_s}{kA\dfrac{\Delta p}{\Delta x}} \tag{3}$$

where m_t is the total mass flow rate, ν is the specific volume of the fluid, and x is the steam quality. The product of these variables is the steam injection flow rate:

$$q_s = x m_t \mu_s \nu_s \tag{4}$$

Similarly, from Equation (2) the water injection flow rate can be derived as:

$$q_w = (1-x)m_t \mu \nu_w \qquad (5)$$

The steam quality is the steam flowing fraction or the mobile part of the steam phase. Hence the water mobile part is the remaining portion of the fraction. The flowing fractions can be obtained by the simultaneous injection of steam and water or by injection of water going through phase change. We have experimented with both injection approaches and we will describe them in more detail in the next sections.

Techniques and/or instruments to measure saturation include the use capacitance probe or gamma ray machines, X-ray computer tomography (CT) scanners, X-ray scanners along with tracers (Oak et al., 1990), microwave scanners (Honarpour and Huang, 1995) and the use of tracers. Among the most accurate is the CT scanner. The accurate determination of fluid saturation in porous media (Johns et al., 1993; Satik et al., 1995), and the ability of a CT scanner to provide images of a core that can be analyzed for homogeneity, fluid segregation and channeling make this an excellent instrument for relative permeability experiments.

To the best of our knowledge, Table 1 summarizes previous work in steam-water relative permeabilities with their respective techniques for measuring saturation. Table 1 includes references to experimental work and to the use of production history to estimate relative permeability. A chronological review of the literature can be found in Sanchez and Schechter (1990), Satik et al. (1995), and Ambusso (1996).

Some of the results from the references in Table 1 are plotted for comparison in Figures 1 through 8. Ambusso (1996), Figure 1, showed a large variation with respect to the nitrogen-water curves shown in Figure 8. Counsil and Ramey (1979), Figure 2, also concluded that steam-water relative permeabilities are different than nitrogen-water relative permeabilities. Verma and Pruess (1985), Figure 3, reported similar results to oil-

water and gas-water noting that the non-wetting (steam) phase had a higher deviation than the wetting phase when compared to two component two phase flows. Contrary to these results Piquemal (1994), Figure 4, and Sanchez and Schechter (1987), Figure 5, found a close relation to their gas-water relative permeabilities that are also shown in Figure 8. It is worth noting that these two last references are the only ones from Table 1 that reported the use of unconsolidated cores in their experiments. Monsalve et al. (1984), Figure 6, and Closmann and Vinegar (1988), Figure 7, measured steam-water relative permeability curves but quantitative comparison is limited by the relatively small range of data presented. Most importantly, Figures 1 through 7 show a clear discrepancy in the measurements of steam-water relative permeabilities. Figure 8 shows also that gas-water relative permeability curves found in the literature are not in agreement with each other. Note that in Figure 8, Piquemal (1994), used air instead of nitrogen for the non-wetting/gas phase.

Table 1: Saturation techniques and core type in different experiments relevant to steam-water relative permeabilities.

Reference	*Year*	*Experiment type*	*Saturation technique*	*Core type*
Ambusso	1996	Steam-water	CT scanner	Berea sandstone
Piquemal	1994	Steam-water	Capacitance probe, (gamma ray)	Unconsolidated quartz sand
Closmann and Vinegar	1988	Steam-water-oil	CT scanner	Natural core
Sanchez and Schechter	1987	Steam-water	Tracer	Unconsolidated sandpack
Verma and Pruess	1985	Steam-water	Improved Densitometer, (gamma ray)	
Monsalve et al.	1984	Surfactant-steam-water	Tracer	Berea sandstone
Counsil and Ramey	1979	Steam-water	Capacitance probe, (gamma ray)	Consolidated synthetic cement
Horne and Ramey	1978	Steam-water	Production history	
Chen et al.	1978	Steam-water	Capacitance probe, (gamma ray)	Consolidated synthetic cement
Grant	1977	Steam-water	Production history	
Trimble and Menzie	1975	Steam-water-oil	Did not measure	Berea sandstone
Arihara	1974	Steam-water	Did not measure	Consolidated core

Hence it is clear that further work was required. The use of a high resolution CT scanner to measure saturation distributions and a modern computer-based data-acquisition system were part of our experimental improvements to obtain more reliable measurements.

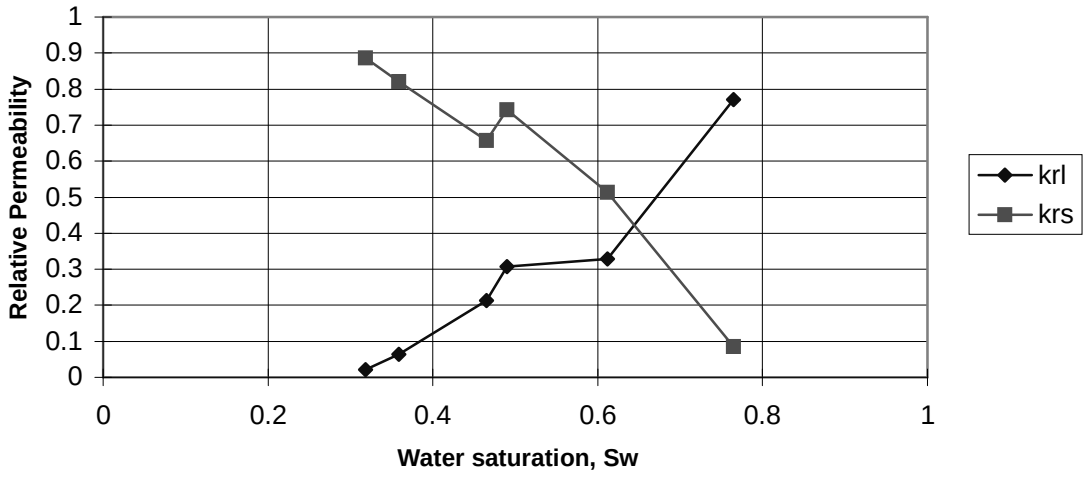

Figure 1: Ambusso (1996), steam-water relative permeability measurements.

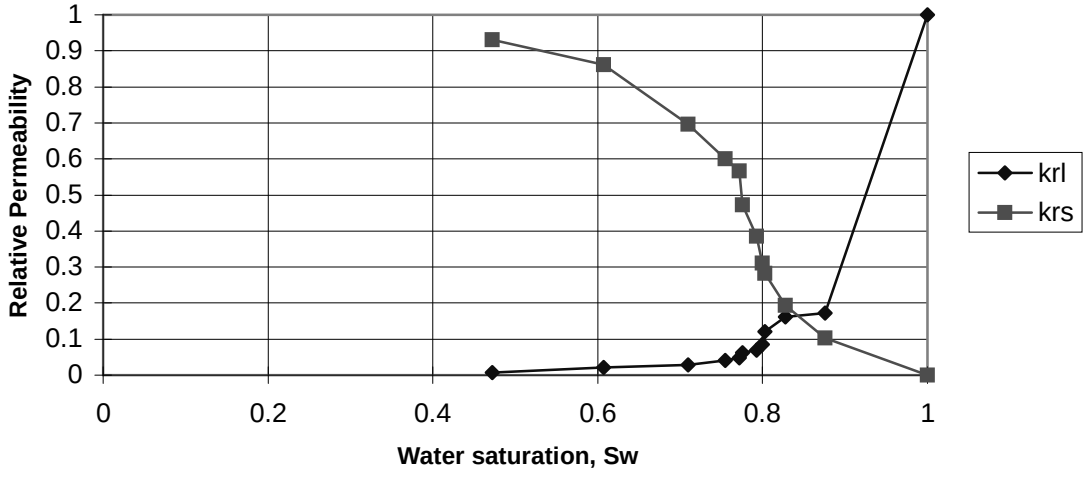

Figure 2: Counsil and Ramey (1979), steam-water relative permeability measurements for low flow rate, run SW2.

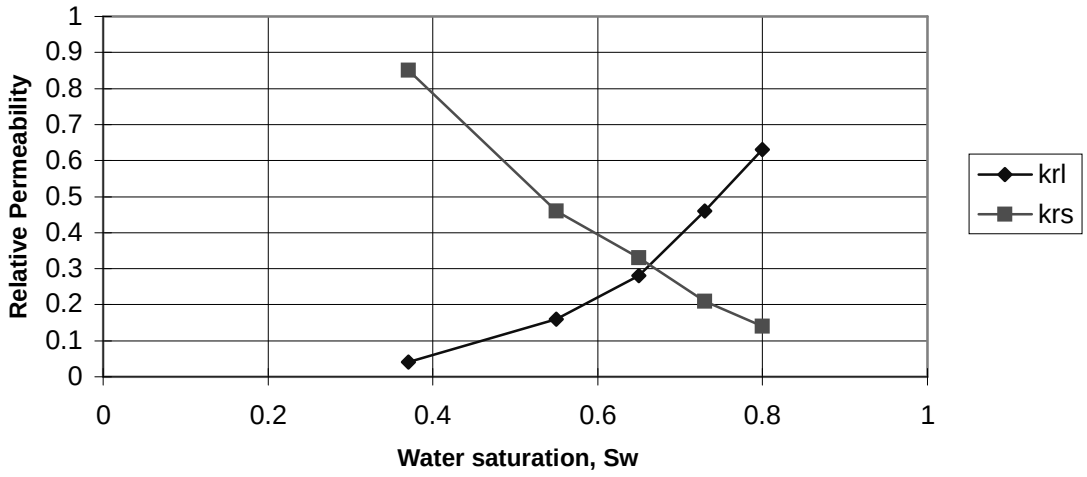

Figure 3: Verma and Pruess (1986), steam-water relative permeability measurements.

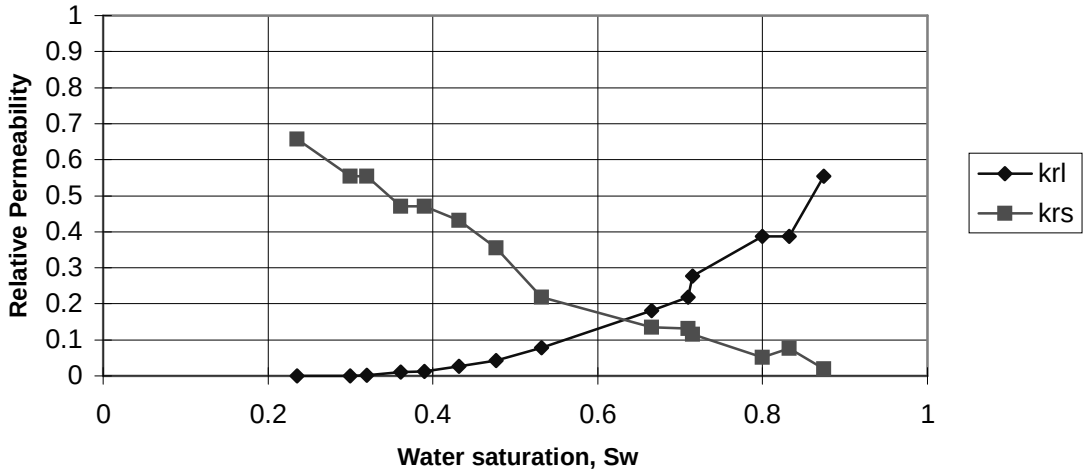

Figure 4: Piquemal (1994), steam-water relative permeability measurements.

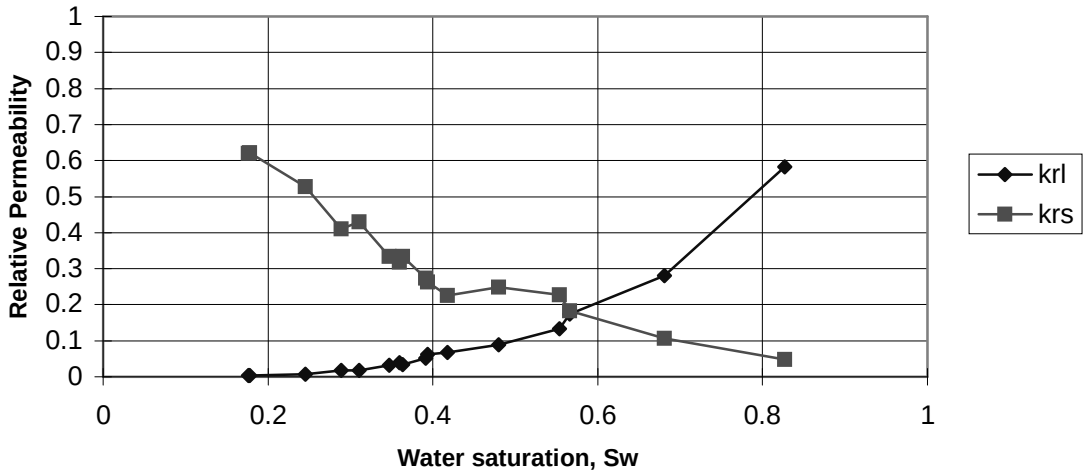

Figure 5: Sanchez and Schechter (1987), steam-water relative permeability measurements.

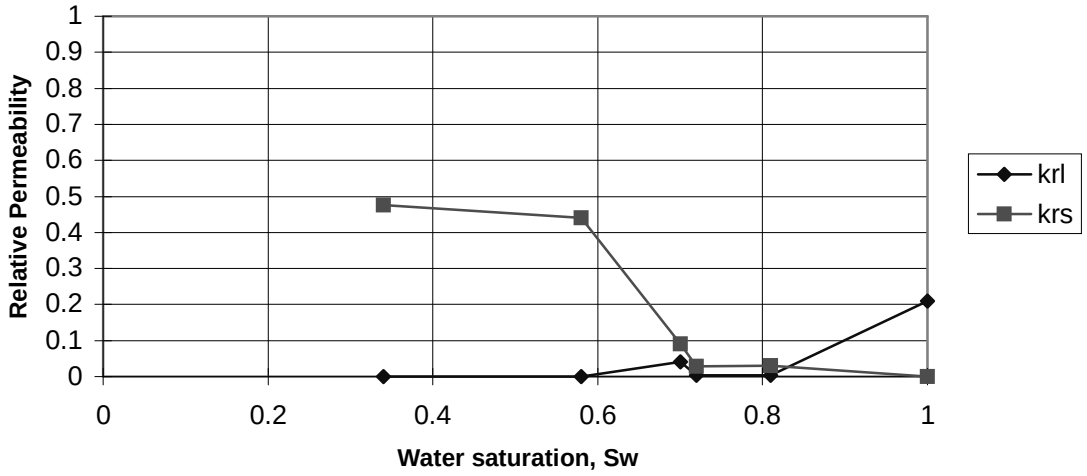

Figure 6: Closmann and Vinegar (1988), steam-water relative permeability measurements.

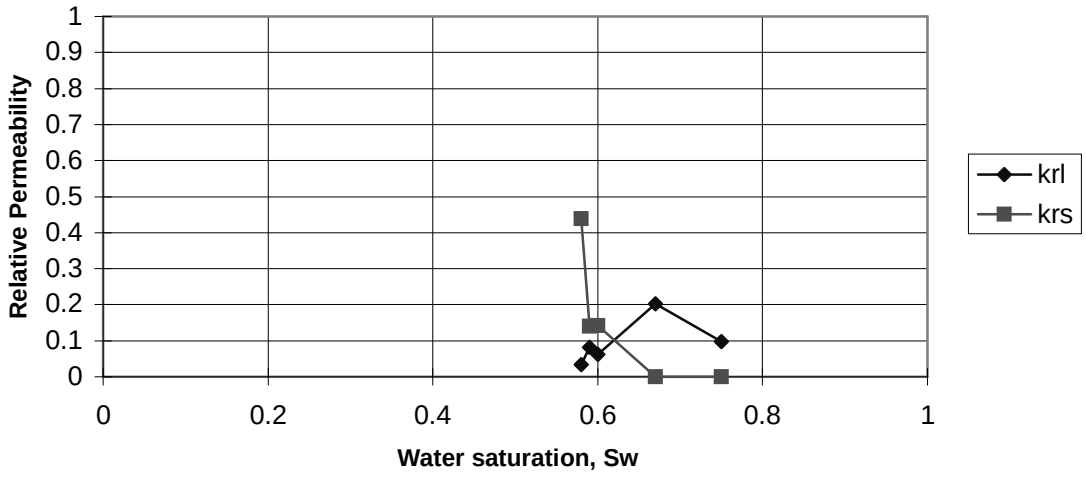

Figure 7: Monsalve et al. (1984), steam-water relative permeability measurements.

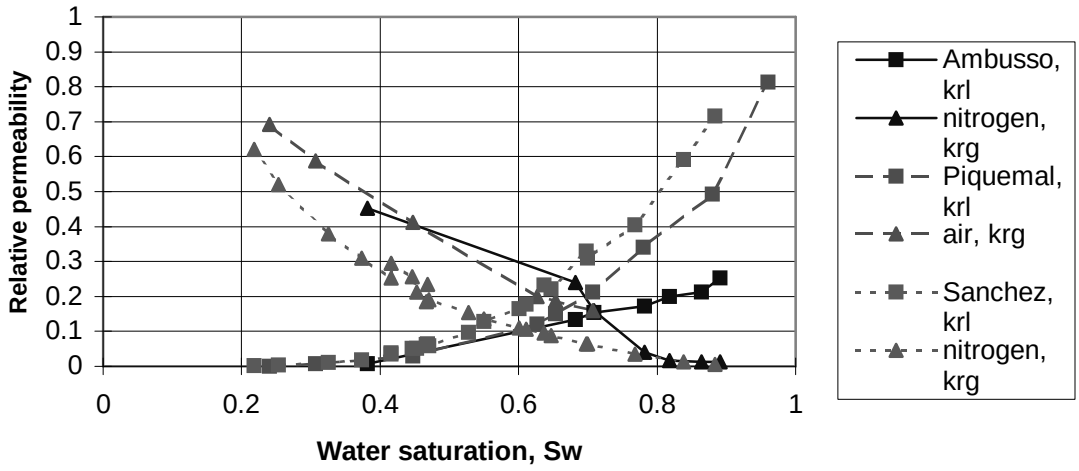

Figure 8: A comparison of gas-water relative permeability measurements by Ambusso (1996), Piquemal (1994), and Sanchez and Schechter (1987).

Section 3

Experimental Apparatus

The experimental apparatus consisted of a CT scanner (Figure 9) and a core holder (Figure 10). The scanner was an X-ray computer tomography device with a resolution of 0.5 millimeter. The scanner measured porosity and in-situ saturation in the core while the experiment was in progress. The scans were obtained at every centimeter along the core when steady-sate conditions were reached. The principles of the use of X ray CT are described in Johns et al. (1993) and a brief summary is given also by Satik et al. (1995).

(a) (b)

Figure 9: Pictures of (a) the core holder and X-ray CT scanner couch and (b) the CT scanner controls used in the experiments.

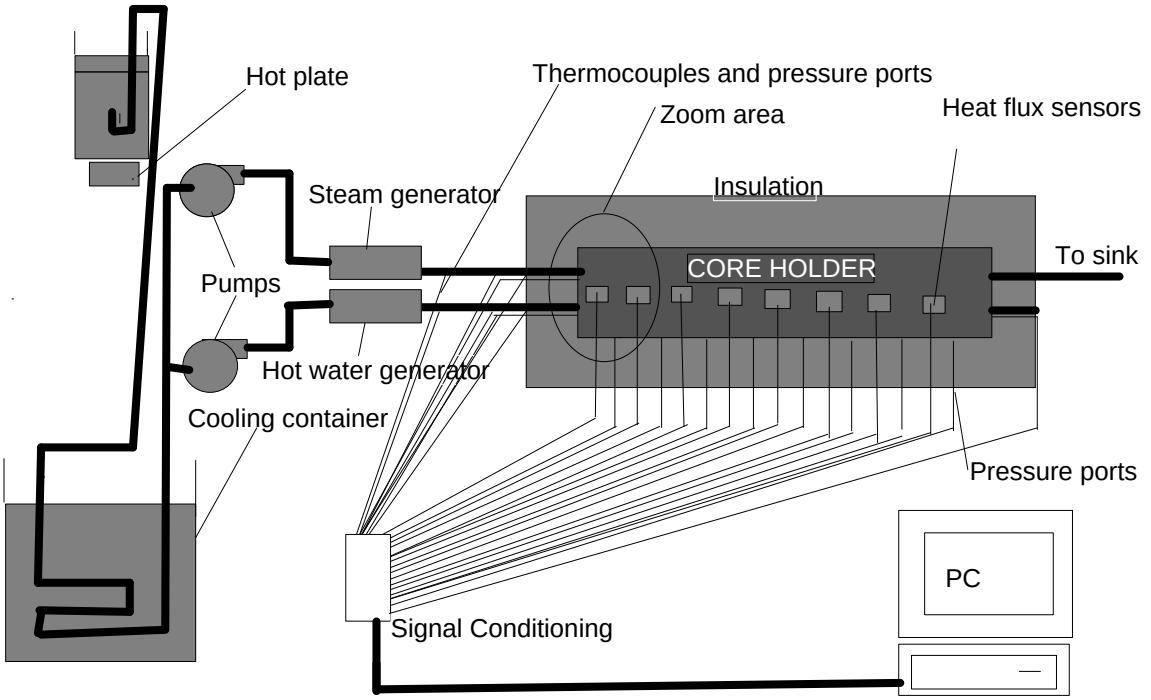

Figure 50: Experimental apparatus for simultaneous injection experiments to obtain steam-water relative permeabilities.

and thermocouples

The samples used were homogeneous Berea sandstone cores 43 cm in length and 5 cm in diameter. Before the experiment, the core sample was heated to 450°C for about twelve hours to deactivate clays and to get rid of any trapped water. The core was then covered with high temperature epoxy (Duralco-4461 manufactured by Cotronics). Eight 1/16" ID Swagelok pressure ports were fixed with epoxy at five centimeter intervals. Injection and production ports (1/8" ID) were also fixed with epoxy at the ends of the core. Detailed explanations of the epoxy preparation, application to the core and difficulties encounter were discussed by Ambusso (1996). Eight Rdf brand micro foil T-type thermocouples/heat flux sensors were installed at the same axial locations as the pressure ports to measure temperature and radial heat losses along the core. The core was tested for leaks before being covered with an insulation material made of ceramic blanket. In addition, nine pressure ports and nine J-type thermocouples were installed in the injection and production lines. The pressure transducers used were Celesco model KP-15 and Custom Electronic Systems, Inc. model 238-FP-10psi-5v-3w. The piping used for the experiments was 1/8" and 1/16" ID Teflon tubing with stainless steel Swagelok fittings.

All lines between the furnaces and the core holder were covered with ceramic blanket to avoid heat losses. Two furnaces were used to generate steam and hot water. The furnaces, steam and hot water generators, had maximum capacities of 1.9 KVA and 1.7 KVA respectively. Two power controllers were used to control the energy supplied by each of the two furnaces. The fluids were injected by two Dynamax SD-200 solvent delivery pumps made by Rainin.

The proportional voltage signals from the heat flux sensors, thermocouples and pressure transducers were first conditioned and then collected in a personal computer by a data acquisition system through an AT-MIO-16DE-10 data acquisition card. The data was then analyzed using "LabVIEW", version 4.0, a graphical programming software by National Instruments. "LabVIEW" used control panels as interactive interfaces for supplying inputs to and observing outputs from the experimental apparatus. The program used a code diagram that contained icons representing input/output operations, computational functions, and analysis functions to organize the program source code. The source code was a modification of a "Temperature Monitor" example program included in the software package. The program monitored temperatures, heat fluxes and pressures on a four chart panel as well as on a panel similar to Figure 10, shown in Figure 11. The program could save the data in spreadsheet form as often as needed, allowing further data processing and analysis. A steam table calculation was used to signal and alert if saturation conditions were reached, which was crucial to this experiment. Heat flux measurements were made using heat sensors that produced an analog output DC voltage of ±10mV. The relationship between voltage and heat flux was directly proportional at constant temperature. For varying temperatures a correction factor chart was provided for each heat sensor by the manufacturer. This chart was interpolated directly within the software code to output real time heat flux in watts per square meter. In addition, the software calculated real time absolute permeability, the flowing fraction of steam and steam-water relative permeabilities.

The signal conditioning hardware consisted of an SCXI-1000 chassis, two SCXI- 1100 multiplexer amplifiers and two SCXI-1300 terminal blocks, all manufactured by National Instruments.

A complete listing of the “LabVIEW” program can be found in the Appendix.

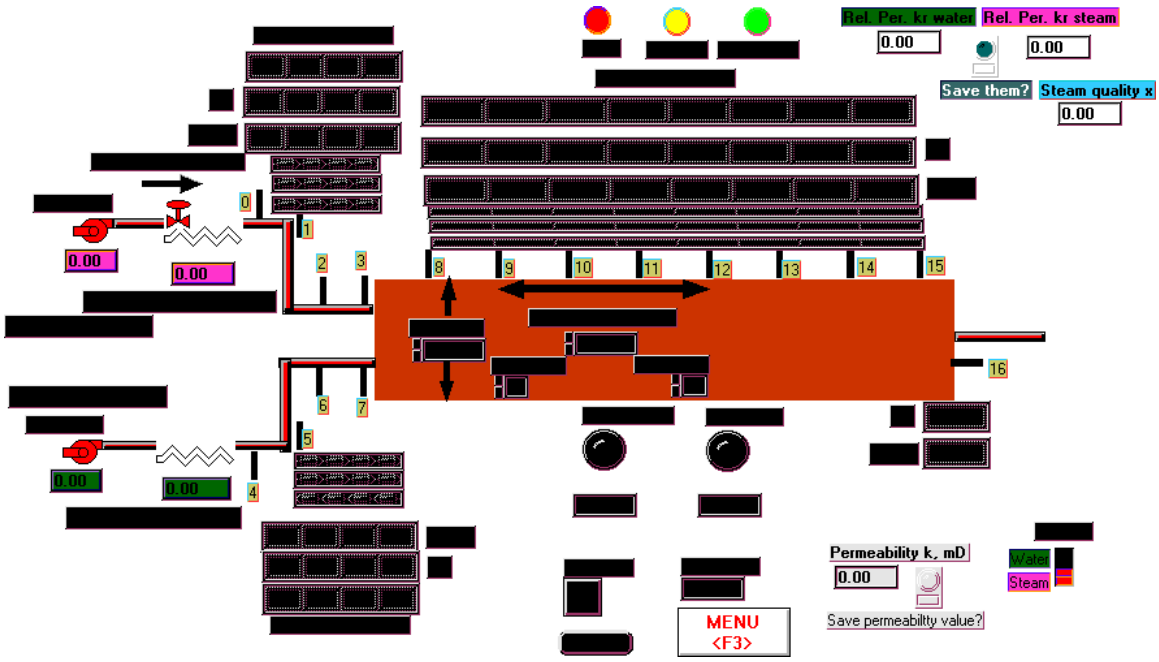

Figure 11: “LabVIEW” control panel.

Section 4

Experimental Procedure

Initially the insulated core holder was secured firmly on the CT scanner couch to ensure scanning of the same locations throughout the experiment. Although heat losses were measured, it was important to insulate the core holder well to obtain sufficiently flat saturation and temperature profiles. Using the vacuum pump, most of the air inside the pore space was evacuated. Under vacuum conditions the core was then scanned along its length to obtain dry CT scan numbers (CT_{dry}).

Deionized water was boiled on a hot plate to remove air initially dissolved in the water that could give erroneous saturation readings (Ambusso, 1996). The water was then passed through a cooling container as shown in Figure 10. Cooling the water was necessary in order to avoid damage to the pump. Cold water at room temperature was injected to the core through the steam generator line. The flow rate depended on the particular core sample inlet pressure. In general, the set ranges varied from 1cc/min to 10cc/min. Once breakthrough was achieved water was allowed to flow for at least a couple of pore volumes to fully saturate the core. Scans were then made to obtain wet CT scan numbers (CT_{wet}) at the same locations as the dry scan had been made. The next step was to prime the lines connecting the pressure ports to the pressure transducers. The steam generator power controller was turned on. Water temperature was increased in steady-state steps. With the pressure transducers primed, absolute permeability was monitored versus temperature. At steady state, once the temperature was at a step close to saturated conditions scans were taken to obtain hot wet CT scan numbers (CT_{hwet}).

Two approaches were studied to obtain relative permeability versus saturation. The first was the simultaneous injection of steam and water to the core using two independent lines. The second was the injection of water through a single line while it underwent a phase change in the furnace. As emphasized in Section 2, the ability to obtain the fractional flow of steam (or water) is crucial in the evaluation of relative permeabilities as the rest of the variables, with the exception of absolute permeability, can be measured directly or can be interpolated from steam tables with the knowledge of fluid temperature. These methods were conceived from the literature described by Ambusso (1996), Piquemal (1994), and Sanchez and Schechter (1987). Independently of the method used, once steady-state was distinguished by constant temperatures and pressures over a period of time, the core was scanned to obtain the corresponding saturated CT scan numbers (CT_{sat}).

Section 5

Calculations and Results

5.1 Porosity

An interpretation software (Fpviewer) was used to evaluate the porosity and saturation distributions from the CT numbers. To calculate porosity the following expression was used (Satik et al., 1995):

$$\phi = \frac{CT_{wet} - CT_{dry}}{CT_{water} - CT_{air}} \tag{6}$$

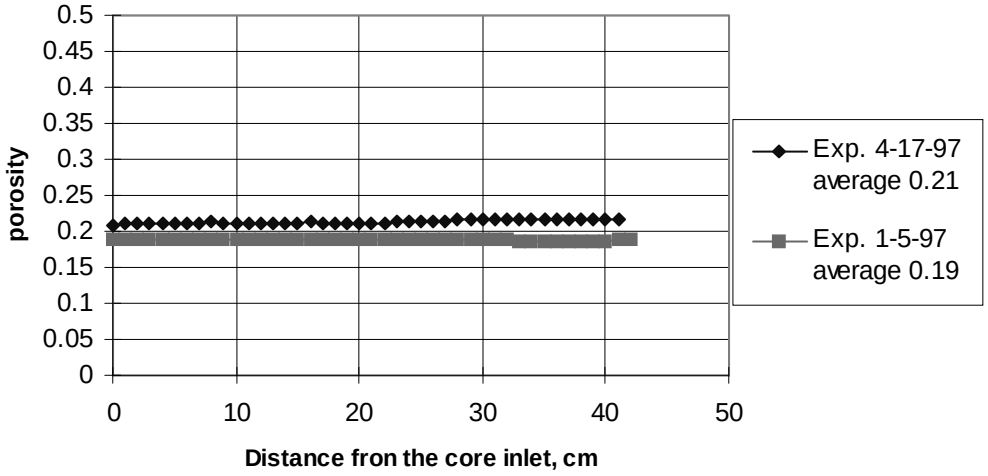

Figure 12: Porosity distributions for two Berea sandstone core samples.

where CT_{water} and CT_{air} are predetermined calibration CT numbers for water and air, respectively.

The average porosity distribution on most of the core samples was about 20%. Each slice was calculated using Equation (6). The porosity distribution along the length of two core samples is plotted in Figure 12. The uniform distribution is consistent with the assumption that the core samples are homogeneous.

5.2 Saturation

Analogous to Equation (6) the steam saturation can be calculated as follows:

$$S_s = \frac{CT_{wet} - CT_{sat}}{CT_{wet} - CT_{dry}} \tag{7}$$

$$S_l = 1 - S_s \tag{8}$$

where S_l and S_s denote liquid water and steam saturations, respectively.

Figure 13 illustrates the steam saturation profile of a core sample taken at a time when the temperature and pressure distributions were as shown in Figure 14 and Figure 15, respectively. The temperature and pressure measurements clearly indicate that no steam can exist along the core. This implies that the values obtained in Figure 13 might be attributed to the variation of liquid density with temperature. Therefore to obtain correct the steam saturation distributions Equation (7) could be modified as follows:

$$S_s = \frac{CT_{hwet} - CT_{sat}}{CT_{hwet} - CT_{dry}} \tag{9}$$

where CT_{hwet} is the scan number taken near saturated conditions and was previously defined as the hot wet scan number. Figure 16 shows CT images at the inlet of the core

obtained using Equations (7) and (9). Figure 17 illustrates the steam saturation profile difference along the core using both equations. This figure demonstrates the error that can be incurred by using cold wet scans. The wet scan must be as close as possible to saturated conditions while being careful not to be in the two-phase zone.

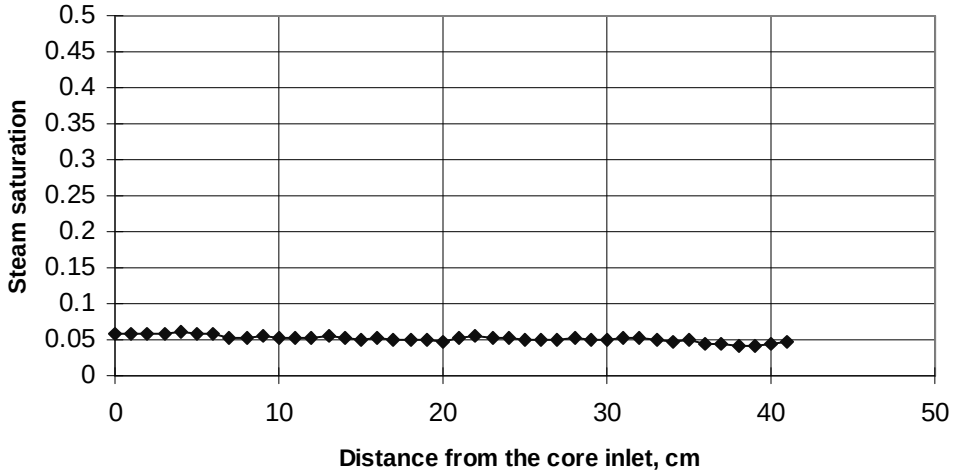

Figure 13: Steam saturation distribution along the length of the core sample from experiment "Exp. 4-4-97".

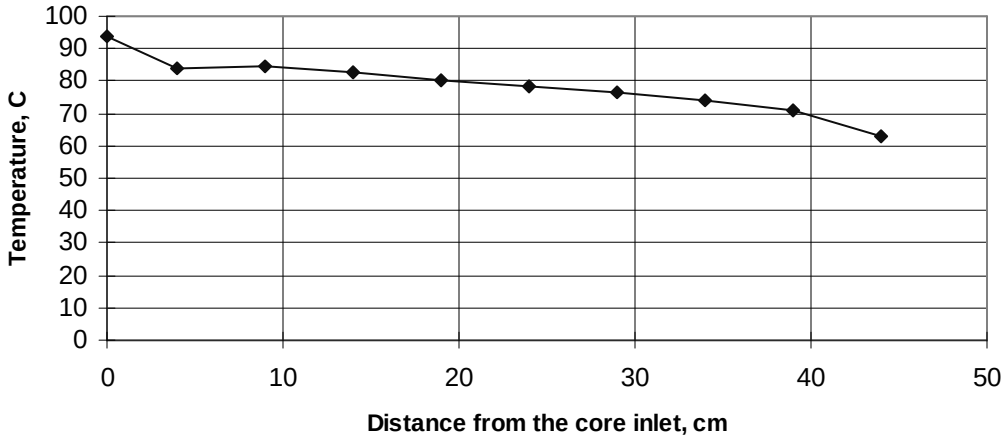

Figure 14: Temperature profile along the core sample from experiment "Exp. 4-4-97".

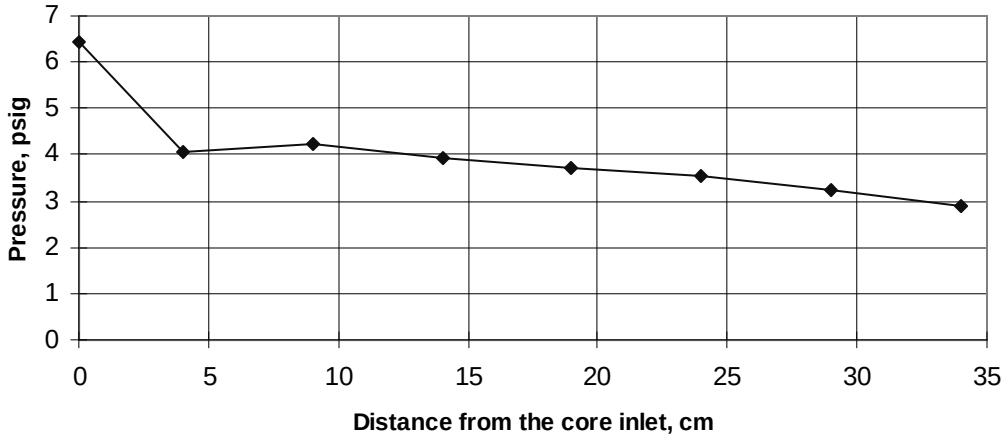

Figure 15: Pressure profile along the core sample from experiment "Exp. 4-4-97".

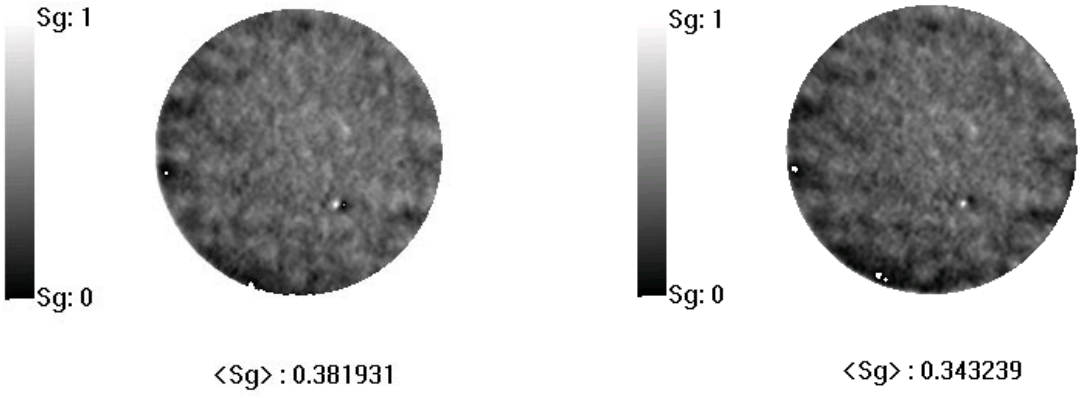

(a) (b)

Figure 16: Saturation distribution images at the core inlet obtained using (a) Equation (7) and (b) Equation (9).

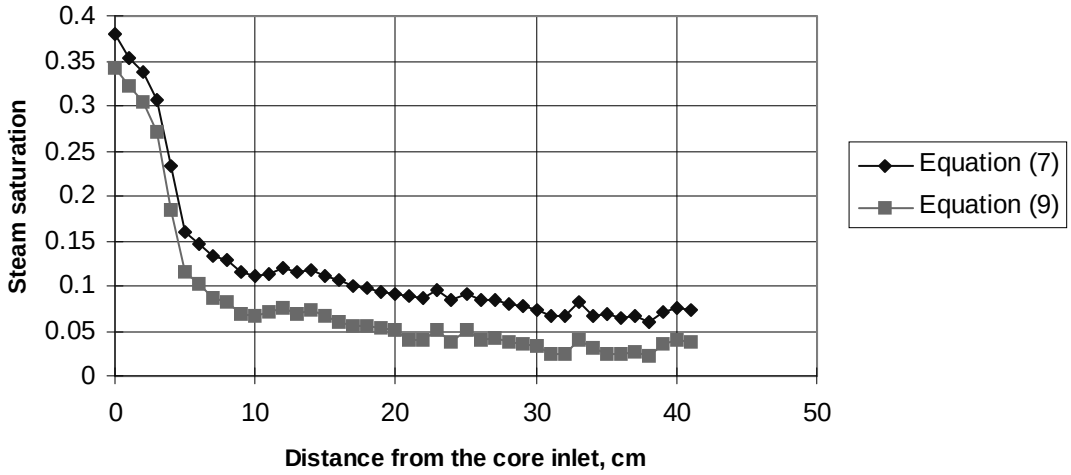

Figure 17: Comparison of two steam saturation profiles along a core sample.

5.3 Absolute permeability

Absolute permeability is evaluated using Darcy's law:

$$k = \frac{\mu q \Delta x}{A \Delta p} \tag{10}$$

where q is the flow rate and the rest of the parameters are defined as in Equations (2) and (3). These parameters can be measured directly with the exception of viscosity. With the appropriate water property table, viscosity can be estimated from fluid temperature measurements.

Experimental results of absolute permeability as a function of temperature are illustrated in Figures 18 to 21. Figure 18 shows absolute permeability measured over a time interval of 250 minutes for the core sample of the experiment labeled "Exp. 12-29-97". Each curve represents measurements at a constant flow rate of 10 cc/min taken at different temperatures of 40^{o}C and 62^{o}C. These curves indicate no major variation in permeability as a function of temperature. Figure 19 shows absolute permeability for core sample of experiment "Exp. 1-5-97".

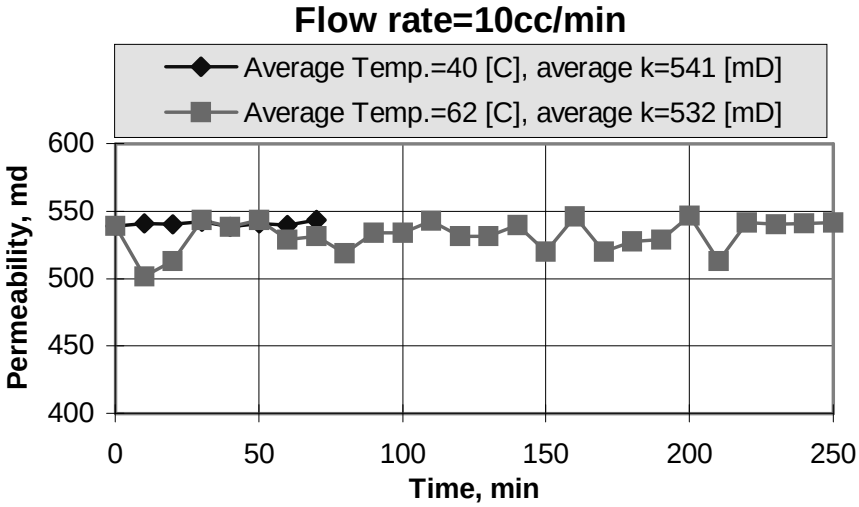

Figure 18: Comparison of permeability at two different temperatures for experiment "Exp. 12-29-96".

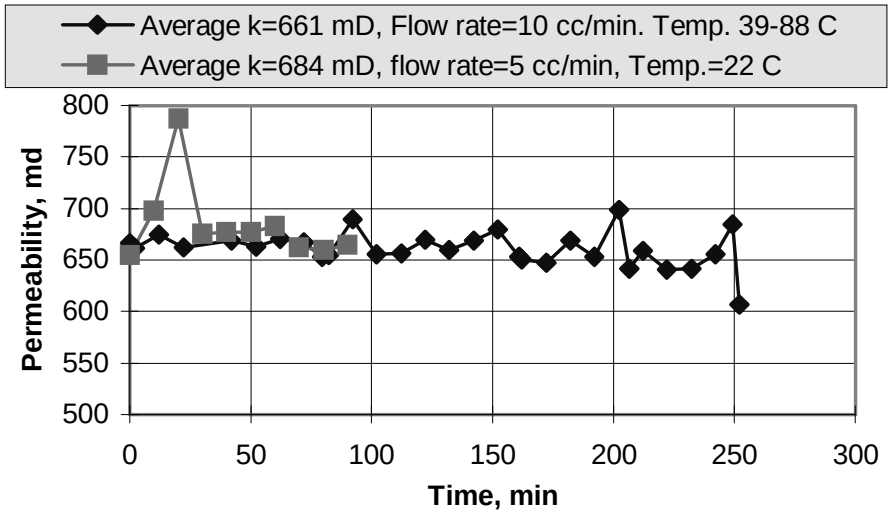

Figure 19: Absolute permeability variation with flow rate and temperature for experiment "Exp. 1-5-97".

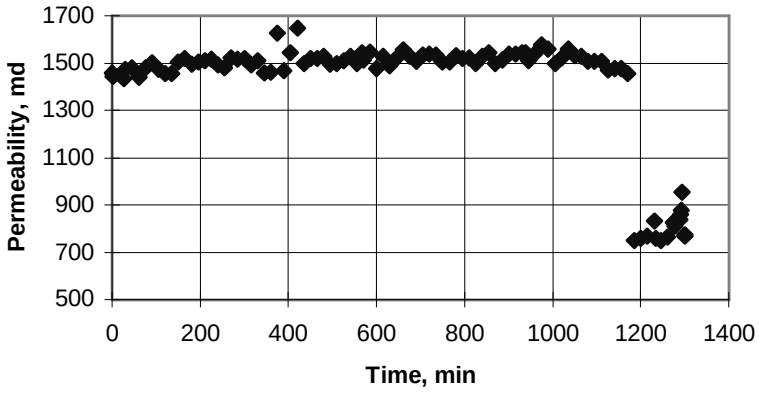

Figure 20: Permeability variation as temperature was increased to 105°C in a period of twenty hours from experiment "Exp. 4-17-97".

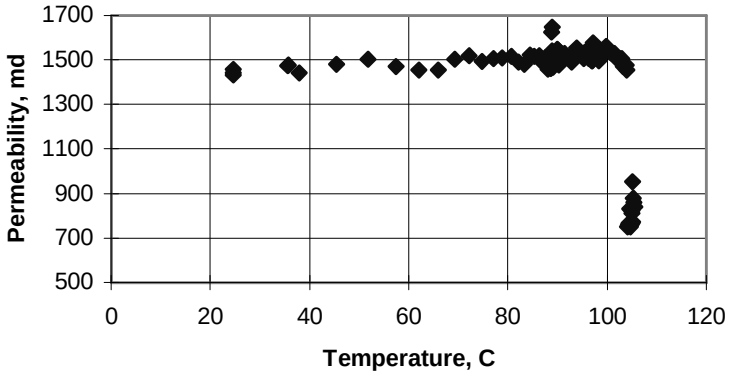

Figure 21: Absolute permeability variation with respect to temperature from experiment "Exp. 4-17-97".

The first curve was measured while the water temperature was increased from 39^{o}C to 88^{o}C at 10cc/min in a period of 250 minutes, and shows only small permeability variation with temperature. The second curve was measured at a constant temperature of 22 ^{o}C and a flow rate of 5cc/min. in a period of 90 minutes. Both curves basically overlap implying a negligible flow rate dependence. Figure 20 and Figure 21 show measurements obtained while the water temperature was increased from 22 ^{o}C to 105 ^{o}C in about 20 hours. The low permeability values of about 900 md are attributed to the onset of two-phase flow

whereas the values were obtained using Darcy's law for single phase flow. These results reveal once again no significant permeability change with respect to temperature.

The literature reports contradictory results on temperature dependence. Trimble and Menzie (1975) reported a permeability increase of 0.23md per °C. On the other hand, according to most of the papers reviewed by Chawathe and Sharma (1991), absolute permeability decreases with increasing temperatures. In addition, Ambusso (1996) reported absolute permeability variations with different flow rates. In general, Figures 18 to 21 indicated only small absolute permeability variations with temperature and flow rate. We believe that such small variations can be attributed to the precision of the pressure transducers and are within experimental error. Small permeability measurements of the order reported by Trimble and Menzie (1975) could not be measured with our experimental apparatus. However for the purpose of this experiment we conclude that permeability variation with temperature and flow rate is negligible.

5.4 Method I: Simultaneous steam and water injection

Mass flowing fractions can be calculated by applying the following mass and energy conservation equations:

$$m_t = m_s + m_l \tag{11}$$

$$m_s h_s + m_l h_l = m_t h_t + Q \tag{12}$$

where m and h denote mass flow rate and enthalpy, respectively and the subscript t refers to total, s to the steam phase and l to the liquid phase. Q is the total heat lost upstream of the point being considered.

To apply these equations to the control volume shown in Figure 22, at point 1, superheated steam was injected at a know rate m_1, pressure p_1 and temperature T_1. At the same time liquid hot water was injected at point 2 at a known rate m_2, pressure p_2 and

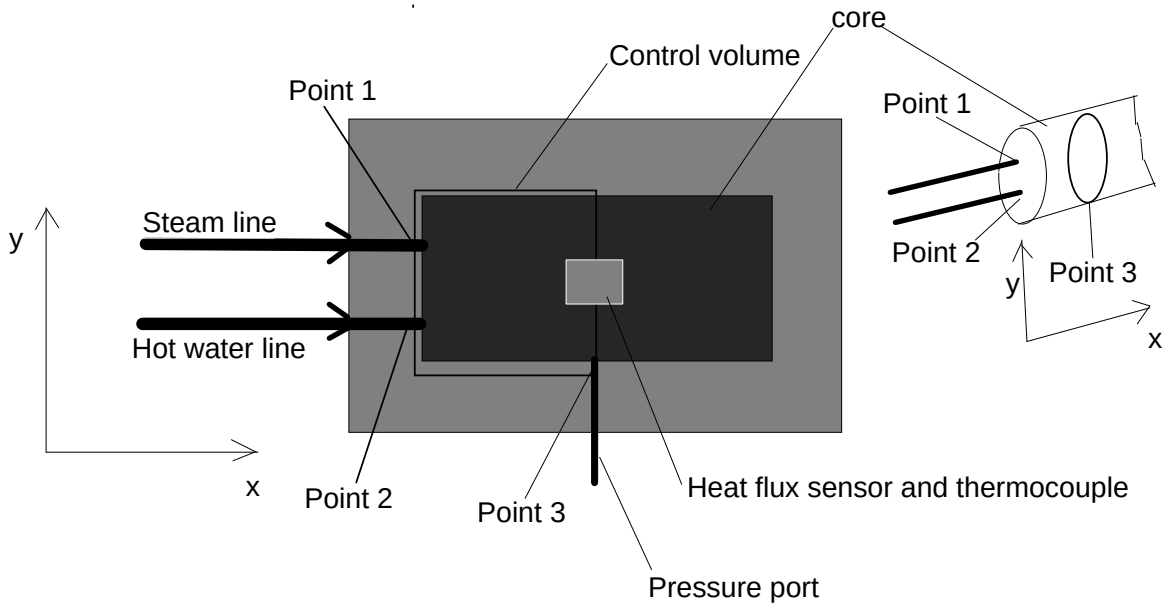

Figure 22: Control volume from Figure 10 zoom area.

temperature T_2. Using a superheated steam table we can interpolate T_1 and p_1 to obtain h_{1s}. Similarly, from a saturated steam table we can approximate h_2 from T_2 by using h_{2l}, the enthalpy at the saturated liquid phase. At point 3, under saturated conditions, from a saturated steam table and using either p_3 or T_3 we can obtain h_{3l} and h_{3ls}, the liquid phase enthalpy and the latent heat of vaporization respectively. Q is obtained by using the measured radial heat flux sensor value Q'':

$$Q = Q'' A_s \tag{13}$$

where A_s is the cylindrical surface area of the core from point 1 (or point 2) to point 3. Substituting in Equation (11):

$$m_3 = m_1 + m_2 \tag{14}$$

and Equation (12):

$$m_1 h_{1s} + m_2 h_{2l} = m_3 h_3 + Q'' A_s \tag{15}$$

where:

$$h_3 = h_{3l} + x h_{3ls} \tag{16}$$

Hence the steam flowing fraction x can be solved to be:

$$x = \frac{m_1 h_{1s} + m_2 h_{2l} - Q'' A_s}{m_3 h_{3ls}} - \frac{h_{3l}}{h_{3ls}} \tag{17}$$

Then the relative permeabilities to steam and water can be calculated for each phase in terms of the mass flow rates by Equations (2) and (3):

$$k_{rl} = -\frac{(1-x) m_t \mu_l \nu_l}{kA \frac{\Delta p}{\Delta x}} \tag{2}$$

$$k_{rs} = -\frac{x m_t \mu_s \nu_s}{kA \frac{\Delta p}{\Delta x}} \tag{3}$$

Figure 23 and Figure 24 show temperature and pressure results from experiment “Exp. 1-5-97”. Figure 23 presents the temperature variation for the steam injection line, liquid water injection line and a point in the core four centimeters downstream of the injection lines.

The injection lines were heated until saturated conditions were reached. At this time heat was added only to the steam line with the hope it would reach superheated conditions. However no matter how much the power to the steam generator was raised it was not possible to confirm that superheated conditions were reached from temperature and

pressure measurements. This is clearly illustrated in Figure 24 where all the measurement readings collapse to one point at saturated conditions. In Figure 23 this is shown by the overlapping of the temperature and pressure measurements. This difficulty was also encountered by Ambusso (1996) and a similar problem in the mixing of steam and water was discussed by Sanchez and Schechter (1987). Ambusso (1996) estimated the steam flowing fraction by extrapolating into the two-phase zone the single liquid phase slope of temperature (enthalpy) versus heat supplied. This implies that heat losses in the two-phase

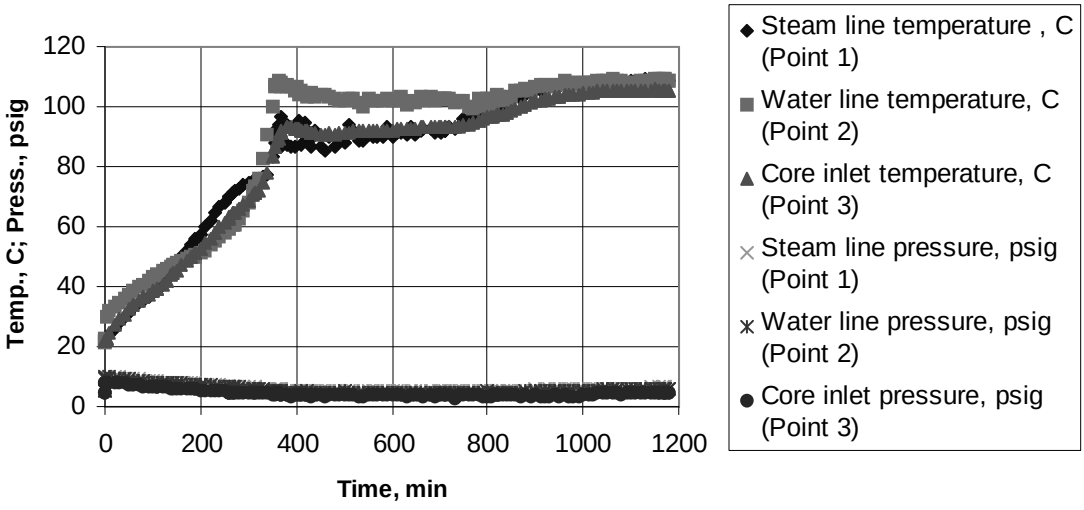

Figure 23: Temperatures and pressures from experiment "Exp. 1-5-97".

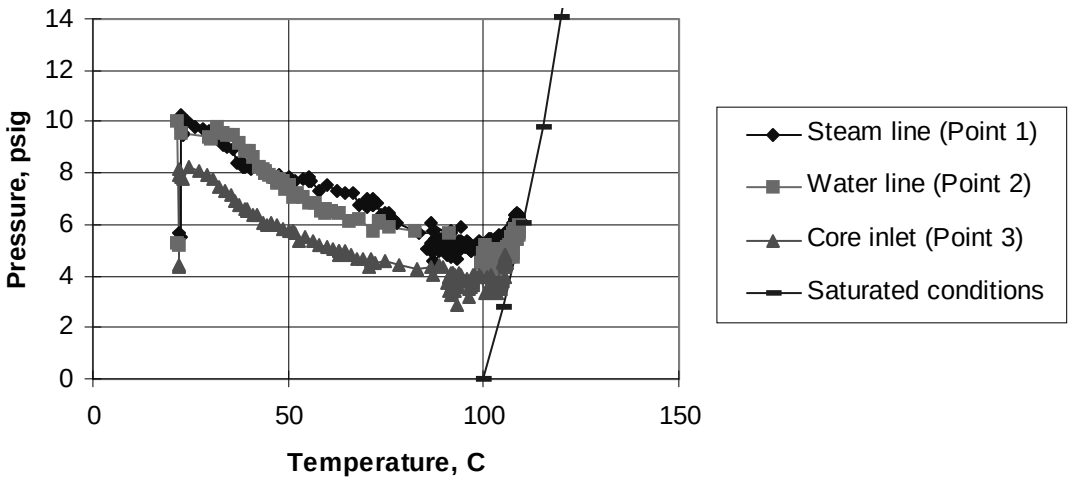

Figure 24: The collapse of data at saturated conditions.

zone are equal to heat losses in the liquid single-phase zone. By making such assumptions, the experiment can be simplified as outlined in the next section.

5.5 Method II: Single injection line

In Method I, the experimental apparatus consisted of an injection unit with two furnaces to generate steam and hot water. However, uncertainty on the injection of superheated steam was a problem. Therefore the design was changed to a similar system with only a single injection unit as shown in Figure 25. The apparatus consisted of one power controller with a variac used to control the heat supplied by the steam generator.

During the experiment, the power of the steam generator was increased in steady state steps. That is, before the power was increased to the next step steady state conditions had to be reached. Initially the water was at subcooled conditions and was slowly brought up to the liquid saturation line. Then the power was raised in steps through the saturation zone until the steam saturation line was reached (Figure 26).

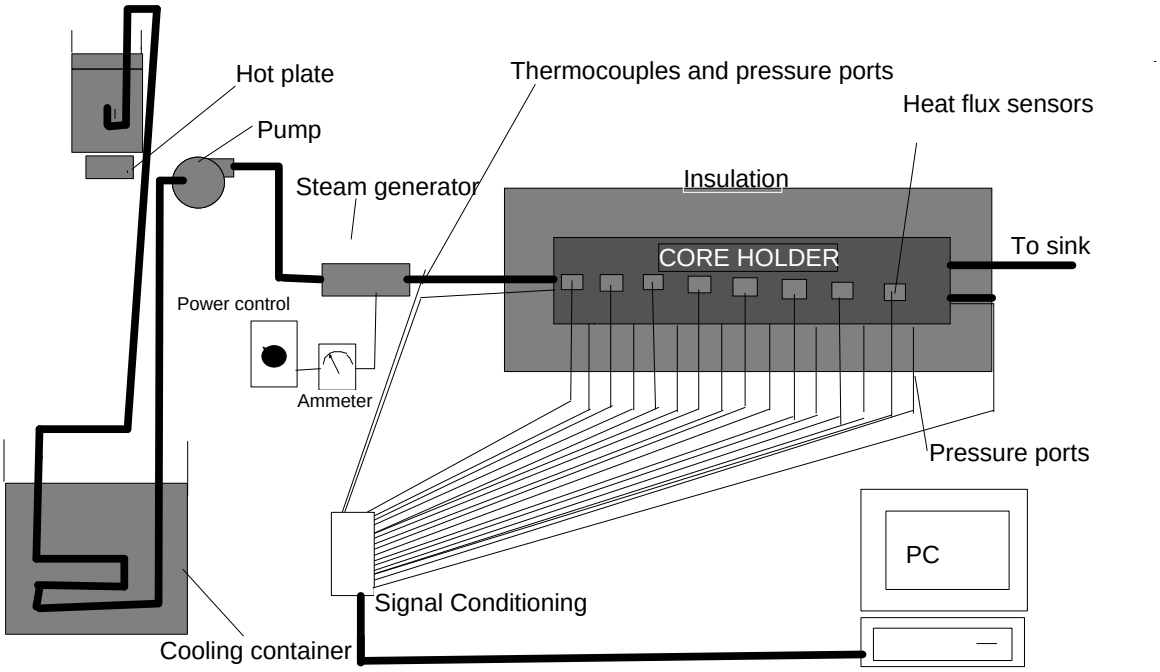

Figure 25: Modified experimental apparatus for single water injection line.

and thermocouples

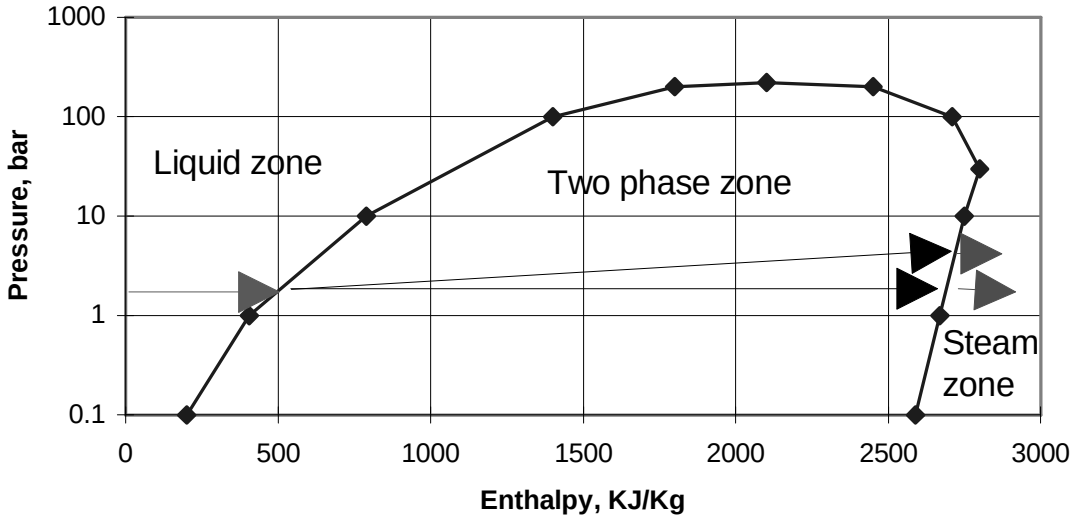

Figure 26: Saturation dome from Cengel and Boles (1989).

Water temperature increased linearly as heat was supplied until the two-phase zone was reached. Once in the two-phase zone the water temperature no longer changed.

However the steam quality increased from zero to one as the heat supplied was increased as shown in Figure 27. At the steam saturation line the steam quality reached its maximum of one and, once again, the fluid temperature should increase linearly with respect to the supplied heat. This method allows us to divide the saturation dome into steps correlated with the heat supplied by the steam generator to obtain the steam mass flowing fractions *x* as follows:

$$power = c + mx \tag{18}$$

where *c* and *m* are constants. Or:

$$amps = c + mx \tag{19}$$

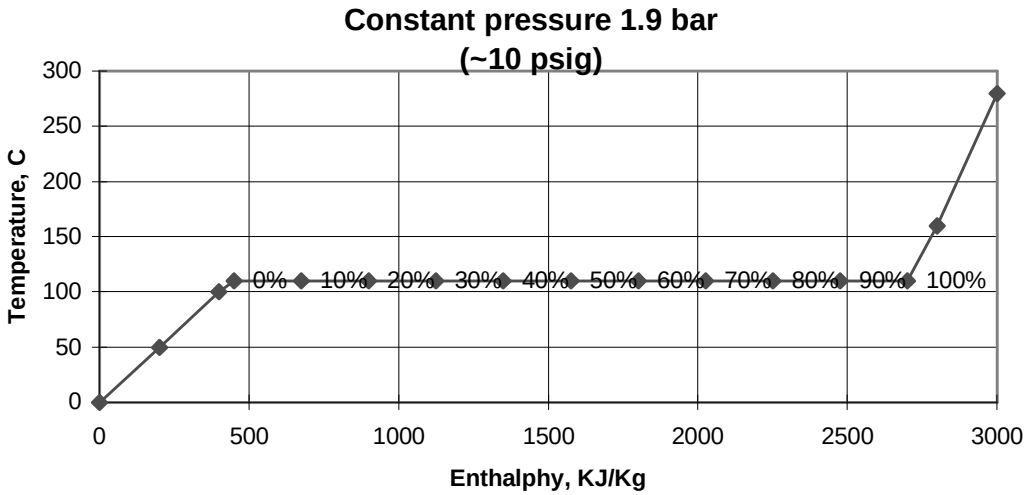

Figure 27: Steam quality increases from zero to one as the heat supplied is increased.

Solving for x we obtain:

$$x = \frac{amps - c}{m} \tag{20}$$

The constants were evaluated at the saturated liquid line where x=0 and at the saturated vapor line where x=1.

As in Method I, the relative permeabilities to steam and water can be calculated with Equations (2) and (3) respectively. This method assumes constant heat transfer rate from the steam generator to the fluid and constant heat losses in the lines throughout the two-phase zone. The advantage of this method with respect to Method I is that it simplifies the experimental apparatus, as well as the procedure and calculations. It is no surprise that two of the most recent experiments to measure steam-water relative permeabilities, Piquemal (1994) and Sanchez and Schechter (1987), used a variation of this single injection technique. Piquemal (1994) calibrated heat losses in the steam generator under conditions of one-phase (liquid) flow while Sanchez and Schechter (1987) used an adiabatic steam generator.

Figure 28 shows data collected in a period of 4630 minutes from experiment "Exp. 4-4-97", illustrating the temperature variation at the core inlet as a function of the heat supplied to the steam generator. The plot eventually flattens at about 300 watts meaning the onset of two-phase flow (saturated liquid, x=0). The peak at about 430 watts could be wrongfully interpreted as the onset of saturated vapor. However, Figure 29 shows a peak in the core inlet pressure at the same power setting implying that the fluid was still in the two-phase zone (Figure 26, inclined arrow line). After the peak the water temperature remains fairly constant up to the end of the experimental data.

Figure 28 and Figure 29 show partial results as the core failed before superheated conditions were reached. In view of this partial agreement between theory and experimental data, Equation (20) is believed to be an adequate estimate of the steam flowing fraction.

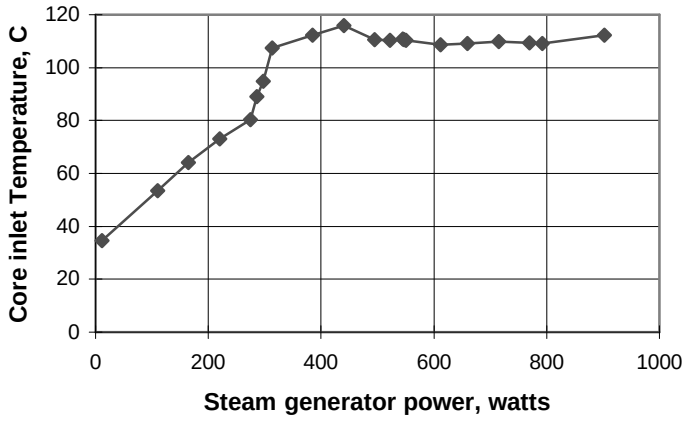

Figure 28: Water temperature versus heat supplied from experiment "Exp. 4-4-97".

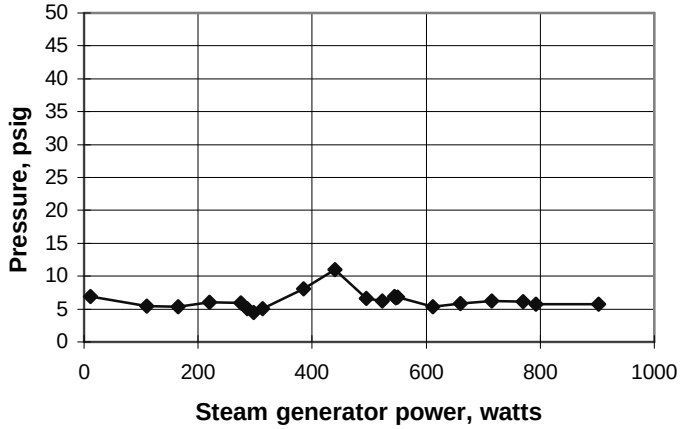

Figure 29: Water pressure versus heat supplied from experiment "Exp. 4-4-97".

It is important to note that with this method as well as with Method I the average steam flowing fraction must be calculated downstream to a point along where the saturation profile is flat. Thus in both cases, Method I and II, this average flowing fraction can be calculated from an energy balance of the downstream radial heat losses.

Section 6
Conclusion

Analysis of the X-ray CT images showed that on the average the core samples were homogenous in porosity.

Considerable care must be exercised to obtain accurate saturation measurements with the X-ray CT scanner. Because of its high resolution, liquid density variation with temperature can be detected, which may give erroneous results in the evaluation of the saturation. Hence for two-phase flow experiments, the scans to compare the liquid phase must be at elevated temperatures as close as possible to saturated conditions. However caution should be taken to avoid reaching the two-phase zone, as this would give even more unreliable saturation measurements.

The variation of absolute permeability as a function of temperature was found to be small. Similarly, absolute permeability measurements remained fairly constant while the water injection flow rate was varied. Small variations can be attributed to the precision of the pressure transducers. From these results, and for the purpose of this experiment, we concluded that absolute permeability does not vary with temperature or flow rate.

Two methods were investigated to obtain steam fractional flows in order to measure relative permeability for steam-water flow in a homogeneous porous medium. The first method was the simultaneous injection of steam and hot liquid water to the core. At steady state, it was difficult to differentiate the conditions between the two injection

fluids. It was also difficult to differentiate the condition of a point downstream of the core injection lines.

The second method, called for the injection of water to while it underwent a phase change. In both methods the heat added or lost could only be approximated, which created uncertainty in the results. The single injection line method is preferred as it simplifies the experimental set up, as well as the procedure and calculations.

Section 7

Nomenclature

A	cross-sectional area of core
A_s	surface area of core
amps	electrical current
c	constant
CT	computer tomography scan number
h	enthalpy
k	absolute permeability
m	mass flow rate
	constant
Q	heat loss
Q”	heat flux
q	volumetric flow rate
S	saturation
x	steam fraction
Δp	pressure drop in the core
Δx	distance along core
ν	specific volume
μ	fluid viscosity
ϕ	porosity

Subscripts

l	liquid phase
g	gas phase
s	steam phase
r	residual
t	total
w	water

Section 8
References

Ambusso W. J., 1976, “Experimental Determination of Steam-Water Relative Permeability Relations,” MS Report, Stanford University, Stanford, California.

Arihara, N., 1974, “A Study of Nonisothermal Single and Two-Phase Flow Through Consolidated Sand Stones,” Ph.D. Thesis, Stanford University, Stanford, California.

Cengel, Y. A., and Boles, M. A., 1989, “Thermodynamics, An Engineering Approach,” McGraw-Hill, New York, New York.

Chawathe, A., and Sharma, M. P., 1991, “Effects of Temperature on the Permeability of Porous Media,” Multiphase Transport in Porous Media, ASME, FED-Vol. 122/HTD-Vol. 186.

Chen, H. K., Counsil, J. R., Ramey, H. J., Jr., 1978, “Experimental Steam-Water Permeability Curves,” GRC Transactions, Vol. 2, pp. 102-104.

Closmann, P. J., and Vinegar, H. J., 1988, “Relative Permeabilities to Steam and Water at Residual Oil in Natural Cores: CT Scan Saturations,” Paper SPE 17449, Presented at the Regional Meeting, Long Beach, California, March, pp. 449-460.

Corey, A. T., 1954, “The Interrelation Between Gas and Oil relative Permeabilities,” Producers Monthly, Vol. 19, pp. 38-41.

Corey, A. T., 1957, “Measurements of Water-Air Permeability in Unsaturated Soils,” Proc. Soil Sci. Soc. Am., Vol. 21, pp. 7-10.

Counsil, J. R., 1979, “Steam-Water Relative Permeability,” Ph.D. Thesis, Stanford University, Stanford, California.

Counsil, J. R., and Ramey, H. J., Jr., 1979, “Steam-Water relative Permeability for Boiling Flow,” Paper SPE 9728.

Dullien, F. A. L., 1979, “Porous Media Fluid Transport and Pore Structure,” Academic Press, New York, New York.

Grant, M. A., 1977, “Permeability Reduction Factors at Wairakei,” presented at the AIChE-ASME Heat Transfer Conference, Salt Lake City, Utah.

Grant, M. A., Donaldson, I. G., and Bixley, P. F., 1982, “Geothermal Reservoir Engineering,” Academic Press, New York, New York.

Honarpour, M. M., and Huang, D. D., 1995, “Simultaneous Measurements of Relative Permeability, Capillary Pressure, and Electrical Resistivity with Microwave System for Saturation Monitoring,” Paper SPE 30540, presented at the Annual Technical Meeting, Dallas, Texas, October.

Horne, R. N., and Ramey, H. J., Jr., 1978, “Steam/Water Relative Permeabilities from Production Data,” GRC Transactions, Vol. 2, July.

Johns, R. A., Steude, J. S., Castanier, L. M., and Roberts, P. V., 1993, "Nondestructive Measurements of Fracture Aperture in Crystalline Rock Core Using X-Ray Computed Tomography," J. Geophys, Res., 98 (B2), pp. 1889-1900.

Monsalve, A., Schechter, R. S., and Wade, W. H., 1984, "Relative Permeabilities of Surfactant/Steam/Water Systems," Paper SPE/DOE 12661, presented at the SPE Symposium on Enhanced Oil Recovery, Tulsa, Oklahoma, April.

Oak, M. J., Baker, L. E., and Thomas, D. C., 1990, "Three Phase Relative Permeability of Berea Sandstone," Journal of Petroleum Technology, pp. 1054-1061.

Osoba, J. S., Richardson, J. J., Kerver, J. K., Hafford, J. A., and Blair, J., 1951, "Laboratory Measurements of Relative Permeability," Petroleum Transaction, AIME, Vol. 192, pp. 147-158.

Piquemal, J., 1994, "Saturated Steam Relative Permeabilities of Unconsolidated Porous Media," Transport in Porous Media 17, pp. 105-120.

Richardson, J. J., Osoba, J. S., Kerver, J. K., and Hafford, J. A., 1952, "Laboratory Determination of Relative Permeability, Petroleum Transaction, AIME, Vol. 195, pp. 187-196.

Satik, C., Ambusso, W., Castanier, L. M., and Horne, R. N., 1995, "A Preliminary Study of Relative Permeability in Geothermal Rocks," GRC Transactions, Vol. 19, pp. 539-543, October.

Trimble, A. E., and Menzie, D. E., 1975, "Steam Mobility in Porous Media," Paper SPE 5571 presented at the 50th Annual Fall Meeting, SPE of AIME, Dallas, Texas, September.

Verma, A., and Pruess, K., 1986, "Enhancement of Steam Phase Relative Permeability Due to Phase Transformation Effects in Porous Media," 11th Workshop on Geothermal Reservoir Engineering, Stanford University, Stanford, California.

Section 9

Appendix

9.1 “LabVIEW” program listing